Field dependence of the magnetization of the two-dimensional antiferromagnet K_2MnF_4

A. F. M. Arts, C. M. J. van Uijen, and H. W. de Wijn
Fysisch Laboratorium, Rijksuniversiteit, Utrecht, The Netherlands
(Received 19 November 1976)

Both the up and down sublattice magnetization and the net magnetization of the nearly two-dimensional antiferromagnet K_2MnF_4 have been measured and analyzed in detail as a function of temperature in external magnetic fields up to the spin-flop transition. The experimental method has been tracking the NMR frequencies of the ^{19}F nuclei adjacent to the magnetic ions. Spin-wave theory with inclusion of Oguchi-type renormalization, as well as semiempirical scaling of the temperature variation of the magnon energy gap, is in excellent agreement with the data up to 18 K for all fields below ~ 40 kG, decreasing to 13 K at 50 kG, i.e., up to a line in the (H,T) diagram where the thermal decrement of the sublattice magnetization is only 7%. Near $T = 0$ K, the spin flop has been observed to occur at 54.5 ± 0.5 kG. Renormalization is found to become increasingly important with field, and apparently its field-dependent part is well described by first-order spin-wave interactions. It appears that in a field the magnetization of the sublattice with the magnetic moments in the direction of the external field initially decreases more rapidly with temperature than is the case in zero field. The effect is due to the preferential excitation of long-wavelength magnons of the low-energy magnon branch, which by virtue of Bogolyubov coupling reside on both sublattices. The reduction of T_N with field has been found to be 1.1 ± 0.5 K at 30 kG and 3.5 ± 0.5 K at 50 kG. Finally, the z component of the transferred hyperfine constant of the in-layer ^{19}F was deduced to be -51 ± 1 MHz.

I. INTRODUCTION

The nearly two-dimensional (2D) antiferromagnet K_2MnF_4 has been the subject of several investigations.[1-5] The reason for this interest is the location of the magnetic ions in perfectly simple quadratic layers, with the interlayer exchange at least several orders of magnitude smaller than the intralayer nearest-neighbor exchange. Combined with the small anisotropy, mainly of dipolar origin, the structure is therefore nearly ideal for experimental verification of theoretical results for the 2D Heisenberg antiferromagnet. In this study, we are particularly interested in the sublattice and net magnetizations with emphasis on the effects of magnetic fields up to the spin-flop transition. The crystal structure provides us here with powerful NMR probes in the form of the ^{19}F nuclei neighboring the magnetic ions and resonating in strong hyperfine fields directly proportional to the magnetic moments residing on the Mn^{2+} ions. In a magnetic field there are three distinguishable ^{19}F sites, those adjacent to the layer, reflecting the magnetizations of the up and down sublattices, and the in-layer ^{19}F sites sensing the imbalance of the sublattices or net magnetization.

A spin-wave analysis in zero field has earlier been presented by de Wijn, Walker, and Walstedt,[4] who found excellent agreement, up to temperatures somewhat less than $\frac{1}{2}T_N$, between the temperature dependence of the sublattice magnetization as derived from NMR experiments and spin-wave theory with incorporation of Oguchi renormalization of the magnon energies.[6] Temperature-dependent renormalization improved the fit only marginally by 3 K, while temperature-independent renormalization could be simulated to a very good approximation by effective values for the exchange and the anisotropy. At the point of breakdown between theory and experiment the magnetization has dropped 7%, added to the 7% decrement due to the zero-point motion, i.e., at a point where the number of magnons excited is still very small.

The purpose of the present investigation is to extend this study to external magnetic fields along the tetragonal c axis, which lift the degeneracy of the magnon branches. In a field, the lower branch will become more heavily populated than the upper branch (at 40 kG, for example, the $k=0$ gaps of the two branches are 2 and 13 K, respectively), resulting in a field-dependent renormalization of the magnon energies in excess to the thermal one. In addition to a discussion of the magnitude of field-dependent renormalization as compared to the unrenormalized case, an objective is to determine to what extent the effects of fields on the magnon energies are properly described by first-order renormalized spin-wave theory, even near the spin-flop transition.

II. EXPERIMENTAL

The sublattice and the net magnetization of a single crystal have been measured by tracking the NMR frequencies of the ^{19}F nuclei adjacent to the magnetic ions. These nuclei resonate in strong transferred hyperfine fields with additional dipolar

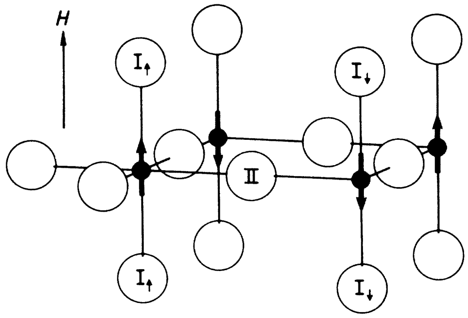

FIG. 1. Various F sites adjacent to the magnetic moments residing on the Mn^{2+} ions in the layer, with the magnetic field parallel to the tetragonal axis. The NMR frequencies of the out-of-layer $^{19}F^{I}_{\uparrow}$ and $^{19}F^{I}_{\downarrow}$ nuclei reflect the magnetizations of the up and down sublattices, respectively, while the NMR frequency of the in-layer $^{19}F^{II}$ sites scales with the net magnetization.

contributions from the magnetic ions in the lattice. With the magnetic field H parallel to the tetragonal axis of the crystal there are three distinct fluor resonances in K_2MnF_4 (Fig. 1). The NMR frequencies of the out-of-layer $^{19}F^{I}$ nuclei $f^{I}_{\uparrow}$ and $f^{I}_{\downarrow}$ reflect the magnetizations of the "up" and "down" sublattices, respectively, while the imbalance of the sublattices is reflected in the frequency f^{II} of the $^{19}F^{II}$ nuclei located between antiferromagnetically coupled Mn^{2+} ions in the magnetic layers. Apart from the shifts due to the magnetizations, the NMR frequencies contain the Zeeman effect of the ^{19}F nuclei. Taking out the latter, the resonance frequencies may be expressed as

$$\Delta f^{I}_{\uparrow}(T,H) = f^{I}_{\uparrow}(T,H) - \gamma H/2\pi = (A_1 + D_1)\langle S^z_{\uparrow}\rangle + D'_1\langle S^z_{\downarrow}\rangle \,, \quad (1)$$

$$\Delta f^{I}_{\downarrow}(T,H) = f^{I}_{\downarrow}(T,H) + \gamma H/2\pi = -(A_1 + D_1)\langle S^z_{\downarrow}\rangle - D'_1\langle S^z_{\uparrow}\rangle \,, \quad (2)$$

$$\Delta f^{II}(T,H) = f^{II}(T,H) - \gamma H/2\pi = (A_2 + D_2)(\langle S^z_{\uparrow}\rangle + \langle S^z_{\downarrow}\rangle) \,, \quad (3)$$

where γ is the gyromagnetic ratio, A_1 and A_2 are the transferred hyperfine constants for the out-of-layer and the in-layer ^{19}F nuclei, respectively, while D_1, D'_1, and D_2 reflect the z components of the dipolar fields of the two sublattices at the various ^{19}F sites. The subscript ↑ refers throughout to the sublattice with the *magnetic moment* pointing in the direction of the applied field, and ↓ to the sublattice with the moment opposite to the field (note that $\langle S^z_{\uparrow}\rangle$ is negative and $\langle S^z_{\downarrow}\rangle$ is positive).

The dipolar fields may be evaluated by direct summation over the lattice, with the following results: $D_1 = -16.5$ MHz (per unit of spin), $D'_1 = 0.22$ MHz, and $D_2 = 9.4$ MHz. Further, the sum $A_1 + D_1 - D'_1$ is accurately known from the zero-field and zero-temperature $^{19}F^{I}$ resonance frequency $f^{I}(0,0) = 150.477 \pm 0.003$ MHz.[4] Combined with the expectation value of S^z at $T = 0$ K, $\langle S^z\rangle = -S + \Delta_0 = -2.330$ with Δ_0 the zero-point spin reduction,[5] this yields $A_1 = -48.33$ MHz, which compares well with $A_1 = -49$ MHz obtained from NMR in the paramagnetic regime.[7] It is further noted from Eq. (1) that $\Delta f^{I}_{\uparrow}$ does not exactly represent $\langle S^z_{\uparrow}\rangle$, but that there is a small contribution of the down sublattice, amounting to $|D'_1/(A_1 + D_1)| = 0.3\%$ only. Analogously, the up sublattice contributes minutely to $\Delta f^{I}_{\downarrow}$.

The NMR frequency has been measured in the frequency range 35–250 MHz by observing the free-induction decay following a high-powered rf pulse with a duration of a few μsec. The detection of the nuclear signal was performed by use of a tunable very-high-frequency receiver, with fast recovery against overload, followed by a double-balanced mixer driven by a standard oscillator. The transmitter as well as the receiver were coupled to the coil wound around the sample through an impedance matching network. There was in general no need for further tuning of the sample coil. The free-induction decays of the ^{19}F resonances at both the I and II sites had a duration of the order of 10 μsec, almost independent of the external field, and decreasing slightly at the higher temperatures.

Below 4.2 K the single crystal was immersed in liquid helium, and temperature stabilization was done by controlled pumping. Above 4.2 K the sample was placed in a continuous stream of boiled-off helium gas, the temperature of which was servo-stabilized to within 0.02 K. In zero magnetic field the temperature was measured with a calibrated germanium resistor, while in a magnetic field use was made of an Allen-Bradley carbon resistor. Corrections, up to 0.09 K, at 50 kG and He temperature, were made for the field-induced change in the resistance value.[8] To check the reproducibility of the carbon resistor calibration points were taken *in situ* before and after every measuring run, but any drift appeared to be minor. The inaccuracy of the temperature is estimated to be 0.03 K in the temperature range up to 20 K, increasing to 0.10 K at 50 K. In the analysis, the inaccuracy of the temperature has been propagated to the error in the frequency. It should be noted here that the accuracy of the $^{19}F^{I}$ data is almost completely determined by the accuracy of the temperature measurements, this in contrast to the $^{19}F^{II}$ data, which are less sensitive to temperature, and where the inaccuracy of the frequency determination is the main cause of the error.

All data were taken with a superconducting solenoid, providing a homogeneous magnetic field

($1:10^5$ over the crystal), and operating in the superconducting mode in view of the required stability of the field over longer periods of time. The field has been measured in two different ways. First, by extrapolating the NMR frequency of the in-layer $^{19}F^{II}$ nuclei to zero temperature, where the imbalance of the sublattices has become zero, and secondly, by observing the NMR frequency of the protons present in the varnish with which the crystal was mounted on the sample holder, at temperatures sufficiently low that demagnetizing effects (see below) vanish. The agreement between both methods appeared to be excellent. It is important, especially in fields near the spin-flop transition, that the c axis of the crystal is properly aligned to the direction of the magnetic field. The simple argument of adding the hyperfine field to the external field shows that a misorientation by a small angle θ leads to a lineshift at the out-of-layer $^{19}F^{I}$ nuclei given by

$$\delta f^{I} = (\gamma H \Delta f^{I}/4\pi f^{I})\theta^2 . \tag{4}$$

By extrapolation to zero temperature, the shift appeared to be only 4 kHz at 20 kG with reference to $f^{I}(T=0,\ H=0) = 150.477 \pm 0.003$ MHz, negligible with respect to the errors in the $^{19}F^{I}$ data beyond 4.2 K from other sources. From Eq. (4) a misorientation of 0.7° is then deduced. The lineshift of the in-layer $^{19}F^{II}$ nuclei due to misalignment is entirely negligible below 30 kG. Above, say, 35 kG the onset of the spin-flop transition at 54.5 kG results in a small shift due to the misalignment, which again has been determined by extrapolation to zero temperature, and has subsequently been corrected for.

We finally have to consider the effects of demagnetizing fields. In case of a homogeneously magnetized slab with dimensions $l\times l$ and thickness d, the demagnetizing field at the center is given by $H_d = -4\pi MN$ with $N = 1-(4/\pi)\arcsin[d^2/2(l^2+d^2)]^{1/2}$, where M is the net magnetization. For our sample $d/l \approx 0.25$, whence $N=0.78$. An *experimental* estimate for N was obtained by observing the proton NMR shift in the varnish at the surface of the sample, which is proportional to $4\pi M(1-N)$ and yields $N=0.8$ for our crystal. With M estimated from spin-wave theory, this results in $H_d \approx 100$ G, or 0.2%, at the largest external fields and temperatures considered, 50 kG and 40 K. This H_d may be neglected entirely in the spin-wave calculations discussed in Sec. III. However, the Zeeman field H occurring in Eqs. (1)–(3) has to be corrected for H_d plus the Lorentz field $\frac{4}{3}\pi M$, or $\approx -4\pi M \times 0.45$, a correction that has been applied to all data presented. At 20 kG and 30 K, for example, the correction to $\Delta f^{I}_{\uparrow}$, $\Delta f^{I}_{\downarrow}$, and Δf^{II} amounts to 60 kHz.

III. SPIN-WAVE THEORY

Before analyzing the data (Sec. IV) we first recapitulate the main results of spin-wave theory with inclusion of Oguchi-type renormalization in an external magnetic field H. The treatment is based on Heisenberg exchange between nearest neighbors, and a small staggered anisotropy field H_A oriented along the preferred magnetic z axis. The antiferromagnetic Hamiltonian then is

$$\mathcal{H} = |J| \sum_{\langle l,m\rangle} \vec{S}_l \cdot \vec{S}_m - g\mu_B (H + H_A) \sum_l S^z_l - g\mu_B (H - H_A) \sum_m S^z_m , \tag{5}$$

with the usual notation ($g_{\pm} = g_e$). In Oguchi's treatment[6] the spin operators $\vec{S}_l$ and $\vec{S}_m$ are expanded by use of the well-known Holstein-Primakoff transformation in products of spin-deviation operators up to first order in $1/2S$. In this approximation the idea of a finite subspace of spin dimensionality $2S+1$ is abandoned, resulting in a neglect of the so-called kinematical interactions. A Fourier transformation expresses the operators in two sets of spin waves, each set being restricted to one of the sublattices. The quadratic part of the Hamiltonian is subsequently diagonalized by a Bogolyubov transformation, mixing the original spin waves $\vec{k}$ dependently in such a way that the new spin waves reside on both sublattices. Finally, renormalization of the energies $E^{(1,2)}_{\vec{k}}$ of the magnons due to spin-wave interactions is calculated as a first-order perturbation in $1/2S$. The result is[9]

$$E^{(1,2)}_{\vec{k}}/4|J|S = [(1+\alpha)^2 - \gamma^2_{\vec{k}}]^{1/2} \mp h \pm (p^{(1)} - p^{(2)}) - g_{\vec{k}}(R_0 + R_1) , \tag{6}$$

with

$$\alpha = g\mu_B H_A / 4|J|S , \tag{7}$$

$$h = g\mu_B H/4|J|S , \tag{8}$$

$$g_{\vec{k}} = (1+\alpha-\gamma^2_{\vec{k}})/[(1+\alpha)^2-\gamma^2_{\vec{k}}]^{1/2} , \tag{9}$$

and where

$$\gamma_{\vec{k}} = \tfrac{1}{4}\sum_{\vec{\delta}} e^{i\vec{k}\cdot\vec{\delta}} \tag{10}$$

is a geometrical factor with $\vec{\delta}$ denoting a nearest-neighbor displacement in the quadratic layer. The quantities R_0 and R_1 are the temperature-independent and temperature-dependent renormalizations, respectively, and read as

$$R_0 = \frac{1}{2SN_0} \sum_{\vec{k}} (g_{\vec{k}} - 1) , \tag{11}$$

$$R_1 = \frac{1}{2SN_0} \sum_{\vec{k}} g_{\vec{k}} (n^{(1)}_{\vec{k}} + n^{(2)}_{\vec{k}}) , \tag{12}$$

where the summations run over the 2D Brillouin zone and the Bose occupation numbers $n_{\vec{k}}^{(1,2)}$ are given by

$$n_{\vec{k}}^{(1,2)} = [\exp(E_{\vec{k}}^{(1,2)}/k_B T) - 1]^{-1}. \tag{13}$$

The renormalization by R_1 appears to be almost independent of field.[9] The terms R_0 and R_1 were derived by Oguchi to describe the effect of the spin-wave interactions in zero field. The term $p^{(1)} - p^{(2)}$ in Eq. (6), with

$$p^{(i)} = \frac{1}{2SN_0} \sum_{\vec{k}} n_{\vec{k}}^{(i)} \quad (i = 1, 2), \tag{14}$$

is additional to Oguchi's result, which applies to the fieldless case. As R_0 and R_1, it constitutes a correction to the spin-wave energies to first order in $1/2S$, but vanishes in zero-magnetic field because of the equal populations of the two branches. While derived here as a higher-order correction to the spin-wave energy of an antiferromagnet, the term appears to be proportional to the imbalance of the sublattice magnetizations [cf. Eq. (18)]. As such, the term may also be regarded, at least to lowest order, as a renormalization with the net magnetization, i.e., calculating the lowest-order spin-wave energies of a ferrimagnet with effective quantum numbers $\langle S_{\uparrow}^z \rangle$ and $\langle S_{\downarrow}^z \rangle$ for the two sublattices. In the classical analogue of sublattice magnetizations precessing in the $k = 0$ mode, the correction $p^{(1)} - p^{(2)}$ may approximately be visualized as a screening of the external field by a factor $(1 - \chi_{\parallel}/2\chi_{\perp})$,[10] where $\chi_{\perp}$ is taken from the molecular-field result. In our calculations we will apply renormalization with field according to Eq. (6).

The magnetizations of the up and down sublattices are given by $M_{\uparrow,\downarrow} = -g\mu_B N_0 \langle S_{\uparrow,\downarrow}^z \rangle$, with

$$\langle S_{\uparrow}^z \rangle = -S + \Delta_0 + \Delta S(T) + \Delta S(H, T), \tag{15}$$

$$\langle S_{\downarrow}^z \rangle = +S - \Delta_0 - \Delta S(T) + \Delta S(H, T). \tag{16}$$

Here, Δ_0 is the zero-point spin reduction ($\Delta_0 = 0.170$ for K_2MnF_4,[5] independent of field),

$$\Delta S(T) = \frac{1}{2N_0} \sum_{\vec{k}} \frac{1 + \alpha}{[(1 + \alpha)^2 - \gamma_{\vec{k}}^2]^{1/2}} (n_{\vec{k}}^{(1)} + n_{\vec{k}}^{(2)}), \tag{17}$$

only weakly dependent on the field through the sum $n_{\vec{k}}^{(1)} + n_{\vec{k}}^{(2)}$, while

$$\Delta S(H, T) = \frac{1}{2N_0} \sum_{\vec{k}} (n_{\vec{k}}^{(1)} - n_{\vec{k}}^{(2)}) \tag{18}$$

reflects the imbalance between the two sublattices.

From neutron diffraction,[3] the renormalization with temperature $-g_{\vec{k}} R_1$ described above proved to be excellent for all $\vec{k}$ except those near $k = 0$. Since the magnon energy gap [cf. Eq. (6) with $k = 0$] is known to decrease with temperature more rapidly than by virtue of $-g_{\vec{k}} R_1$ alone, the consequence of expressing the anisotropy as a staggered field H_A is to take H_A to vary with temperature. For a lattice with tetragonal symmetry it has been derived[11,12] that in case of dipolar anisotropy and in the limit of low temperatures H_A scales with the square of the sublattice magnetization. However, since the magnon energy gap has actually been determined by antiferromagnetic resonance up to 40 K,[9] we preferred to adopt the *experimental* variation of H_A with temperature, as derived from the antiferromagnetic-resonance experiments with essentially the same spin-wave description as used here.

It has earlier been discussed that the effect of the temperature-independent renormalization $-g_{\vec{k}} R_0$ on the calculated magnetization may equally well be described by omitting this term in Eq. (6), and replacing J and α by effective parameters $J_s = J(1 - R_0)$ and $\alpha_s = \alpha/(1 - R_0)$.[4] One objective of the analysis is to see the effects of temperature- and field-dependent renormalization. The results of renormalized theory will therefore be compared with the results of calculations based on the *un*renormalized theory, i.e., Eq. (6) with all renormalizing terms removed, but with the effective J_s and α_s in order to compensate for the effect of omitting $-g_{\vec{k}} R_0$.

In the computer evaluations, for given J and α the self-consistent set of Eqs. (6)–(14) is solved in an iterative way. Then, all constants in the dispersion relation being known, the sublattice and net magnetization are calculated by inserting the Bose occupation numbers in Eqs. (17) and (18). It is emphasized at this point that the evaluation of the summations over the 2D Brillouin zone has been done rigorously by making use of the relation

$$N_0^{-1} \sum_{\vec{k}} F(\gamma_{\vec{k}}) = \frac{4}{\pi^2} \int_0^1 dz\, K((1 - z^2)^{1/2}) F(z). \tag{19}$$

Here

$$K(m) = \int_0^{\pi/2} dx (1 - m^2 \sin^2 x)^{-1/2}$$

is a complete elliptic integral of the first kind. Near $z = 0$ (i.e., the Brillouin-zone boundary), where $K((1 - z^2)^{1/2})$ diverges, the integral may be evaluated as ($\epsilon \leq 10^{-4}$)

$$\int_0^{\epsilon} dz\, K((1 - z^2)^{1/2}) F(z) \approx [(\ln 4 + 1)\epsilon - \epsilon \ln \epsilon] f(0). \tag{20}$$

IV. ANALYSIS OF DATA

In this section the NMR measurements at the $^{19}F^{I}$ and $^{19}F^{II}$ sites will successively be discussed.

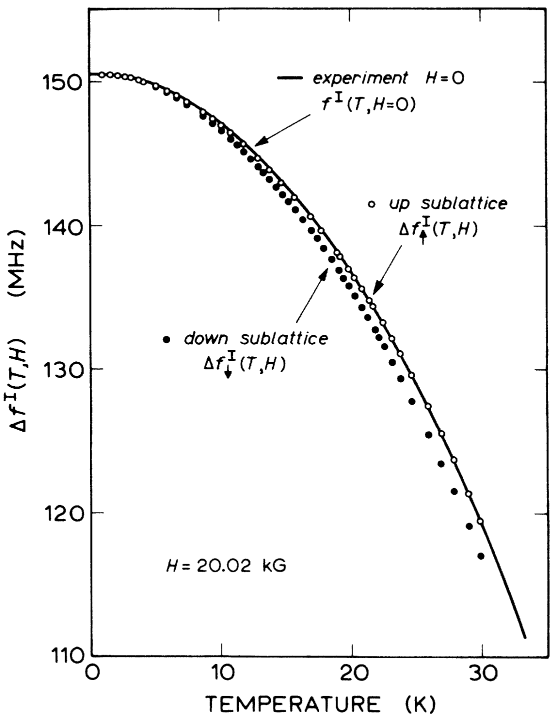

FIG. 2. Resonance frequencies after subtracting the Zeeman shifts $\Delta f^{\mathrm{I}}_{\uparrow}(T,H)$ and $\Delta f^{\mathrm{I}}_{\downarrow}(T,H)$ vs the temperature at 20.02 kG parallel to the *c* axis, reflecting the temperature variation of the up- and down-sublattice magnetizations, respectively. For comparison, the experimental zero-field result has been included as the solid line. Note that on the scale of the figure the difference between $\Delta f^{\mathrm{I}}_{\uparrow}$ and the zero-field data is not resolved.

For the calculation of the magnetizations from spin-wave theory, to which the data will be compared, values for several parameters are required, viz., the hyperfine constants A_1+D_1, D_1', and A_2+D_2 [see Eqs. (1)–(3)], and the spin-wave quantities J and $T_G(0)=E_{k=0}/k_B$, the magnon energy gap at zero temperature (and zero field). The quantities A_1+D_1 and D_1' have already been discussed in Sec. II; A_2+D_2, necessary for the $^{19}F^{\mathrm{II}}$ data, is unfortunately not known to sufficient accuracy, and will therefore be handled below as an adjustable parameter. Although various values of J and $T_G(0)$ are known in the literature, we have preferred here to use the values obtained from least-squares fitting of the temperature dependence of the sublattice magnetization in zero magnetic field to the renormalized spin-wave theory summarized in Sec. III. Such an analysis has been reported by de Wijn, Walker, and Walstedt,[4] but to be sure of consistency with the present experimental conditions, in particular the calibration of the temperature and the use of another sample, we repeated measurements and analysis in zero field. The fit to our data extends to essentially the same upper temperature of 18 K, and yields $J/k_B=-8.40\pm0.05$ K, $T_G(0)=7.55\pm0.04$ K, and a zero-temperature resonance frequency $f(0)=150.477\pm0.003$ MHz. These values are in excellent agreement with those of Ref. 4, $J/k_B=-8.41\pm0.06$ K, $T_G(0)=7.54\pm0.07$ K, and $f(0)=150.477\pm0.003$ MHz. The variation of the sublattice and net magnetization with temperature and field has been calculated with the present values of the parameters.

To indicate the general characteristics of the temperature dependence of the sublattice magnetization in a field, the resonance frequencies $\Delta f^{\mathrm{I}}_{\uparrow}$ and $\Delta f^{\mathrm{I}}_{\downarrow}$ at 20.02 kG are compared to the zero-field experiments (solid line) in Fig. 2. Above 20 kG the resonance has not been followed because of the limited frequency range of the spectrometer and the onset of broadening of the line. It is observed that the down sublattice magnetization decreases more rapidly with temperature. The up sublattice magnetization, on the other hand, closely follows the zero-field dependence. However, detailed inspection reveals that also the up sublattice magnetization at first drops below the zero-field result (this is not resolved on the scale of Fig. 2), contrary to what one would expect from a molecular-field approach.

A. Down sublattice magnetization

The effect of an external field on the sublattice magnetization of the down moments is shown to better advantage in Fig. 3, where $\Delta f^{\mathrm{I}}_{\downarrow}(T,H)$ is plotted relative to the zero-field resonance frequency $f^{\mathrm{I}}(T,H=0)$, with the latter deduced from the *experimental* data points by interpolation with a smoothed cubic spline. The maximum field-induced effect observed amounts to ~−2.5 MHz at 20 kG and 30 K. In Fig. 3, the combined error of $\Delta f^{\mathrm{I}}_{\downarrow}(T,H)$ and $f^{\mathrm{I}}(T,H=0)$ is estimated to be ~20 kHz at the lowest temperature, increasing to ~100 kHz at 30 K. The solid curves in Fig. 3 have been calculated with the renormalized spin-wave theory as described in Sec. III. Here, $\Delta f^{\mathrm{I}}_{\downarrow}(T,H)-f^{\mathrm{I}}(T,H=0)$ has been obtained by subtracting the calculated frequency in a field from the corresponding *calculated* zero-field result, so that a comparison with the experimental data points in Fig. 3 provides a test of spin-wave theory with special emphasis on the *field* effects. The agreement is excellent for all fields up to temperatures of, say, 22 K. However, the experimental data on $\Delta f_{\downarrow}(T,H)$ themselves already deviate from spin-wave theory at 18 K. It is noticed at this point that no adjustable parameters have been used, but instead parameters have been taken from other sources, as discussed above. In terms of

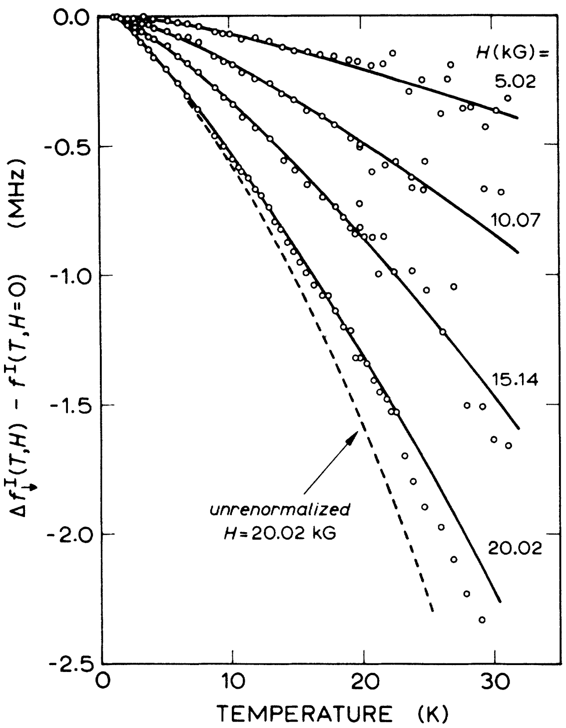

FIG. 3. NMR frequency of the $^{19}F_{\downarrow}^{I}$ nuclei corrected for the Zeeman shift $\Delta f_{\downarrow}^{I}(T,H)$ relative to the experimental NMR frequency in zero field $f^{I}(T,H=0)$ vs temperature, i.e., the temperature variation of the field-induced part of the down-sublattice magnetization. The various fields are parallel to the c axis. The solid lines have been calculated from renormalized spin-wave theory, as described in text. The dashed line refers to 20.02 kG, but has been calculated from unrenormalized theory with effective parameters J_s and α_s.

unrenormalized theory with effective parameters (see Sec. III), however, the sublattice magnetization can only be described up to temperatures steadily decreasing with increasing magnetic field. At 5 kG, there is a reasonable agreement up to 15 K, but at 20 kG (dashed curve in Fig. 3) the match with experiment extends to only 10 K. Because the temperature-dependent renormalization R_1 is almost independent of the magnetic field, the conclusion is that the improvement by renormalization almost completely originates from the field-dependent part $p^{(1)} - p^{(2)}$.

Before turning our attention to the up sublattice, we first discuss residual effects arising from exchange coupling between nearest-neighbor layers. Because of the staggered registry of the magnetic moments in these layers, the exchange interactions of magnitude J' between adjacent magnetic ions located in adjoining layers cancel in zero field. However, in a field when $|\langle S_{\uparrow}^{z}\rangle| \neq |\langle S_{\downarrow}^{z}\rangle|$, there will be a net interaction, which in terms of the molecular-field approximation may be expressed as a static temperature-dependent field related to the imbalance between the sublattices, i.e., $H_E' = 8J'\Delta S(T,H)/g\mu_B$, which adds to the external field at the Mn sites (note that the effect on the F sites is already comprised in the dipolar hyperfine fields). For the exchange coupling between *next*-nearest-neighbor layers, involving many exchange paths, an upper limit of 4×10^{-4} of the primary exchange has been deduced,[4] from which an upper limit for $|J'/J|$ may be set at, say, 1%. Then, with $\Delta S(T,H) \sim 0.01$ at 20 kG and 20 K, $H_E' \sim 0.05$ kG, which is far below the level of detection in Fig. 3.

B. Up sublattice magnetization

From the physical point of view the results for the magnetization of the up sublattice are more elucidating. The experimental data have been plotted in Fig. 4, again with reference to the experimental zero-field frequency, where it is noticed that a *positive* frequency shift corresponds

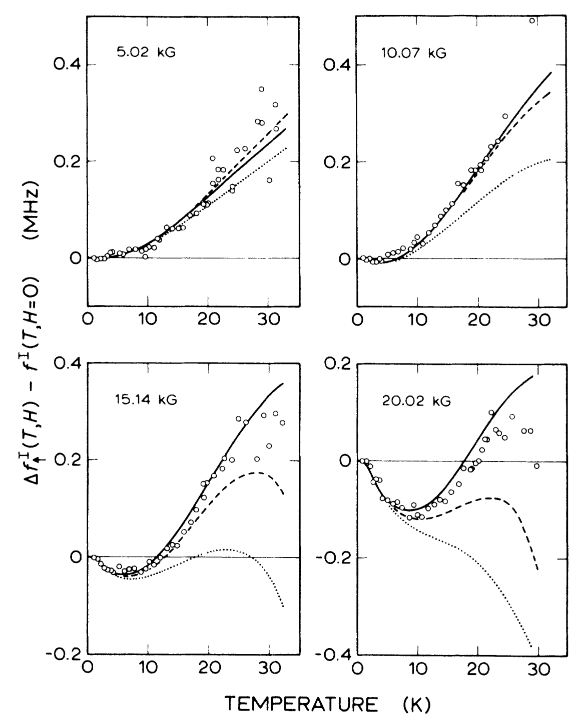

FIG. 4. Same as Fig. 3, but for the up sublattice. The solid lines have again been calculated from renormalized spin-wave theory. The dashed curves, which represent unrenormalized theory with effective parameters J_s and α_s, show the improvement by renormalization, while the dotted lines are computations in the k^2 approximation. The sign reversal as a function of temperature originates from Bogolyubov coupling of the sublattices through long-wavelength magnons.

to an *increase* of the sublattice magnetization in a field with respect to the magnetization in zero field.

In order to interpret the results it is necessary to recall some properties of the Bogolyubov transformation diagonalizing the Hamiltonian (Sec. III). This transformation mixes the spin waves defined on the two sublattices to two new sets according to

$$\alpha_{\vec{k}}^{\mp}=u_{\vec{k}}^{\mp}a_{\vec{k}}^{\mp}+v_{\vec{k}}^{\mp}b_{\vec{k}}^{\dagger},\quad \beta_{\vec{k}}^{\mp}=v_{\vec{k}}^{\mp}a_{\vec{k}}^{\dagger}+u_{\vec{k}}^{\mp}b_{\vec{k}}^{\mp}, \tag{21}$$

where $a_{\vec{k}}^{\mp}$, $b_{\vec{k}}^{\mp}$ and $\alpha_{\vec{k}}^{\mp}$, $\beta_{\vec{k}}^{\mp}$ are the original and the new magnon operators, respectively, and the coefficients $u_{\vec{k}}^{\mp}$ and $v_{\vec{k}}^{\mp}$ are given by

$$u_{\vec{k}}^{\mp}=\left(\frac{D+(D^2-\gamma_{\vec{k}}^2)^{1/2}}{2(D^2-\gamma_{\vec{k}}^2)^{1/2}}\right)^{1/2}, \tag{22}$$

$$v_{\vec{k}}^{\mp}=\left(\frac{D-(D^2-\gamma_{\vec{k}}^2)^{1/2}}{2(D^2-\gamma_{\vec{k}}^2)^{1/2}}\right)^{1/2}, \tag{23}$$

with $D=1+\alpha$. For the appropriate $\alpha\approx 4\times10^{-3}$, the mixing is almost complete for the $k=0$ magnon, whereas at the zone boundary a spin wave is restricted to either one of the sublattices (at the zone boundary $u_{\vec{k}}^{\mp}=1$ and $v_{\vec{k}}^{\mp}=0$).

The essential point is that at low temperatures the long-wavelength magnons of the low-lying branch $E_{\vec{k}}^{(1)}$ are predominantly populated, which gives rise to concurrent diminutions of both the up and down sublattice magnetizations. Since $E_{k=0}^{(1)}$ is below the zero-field gap, the decrease with temperature will be faster than in zero field, as indeed has been observed (Figs. 3 and 4). However, when the temperature is raised, also short-wavelength magnons of $E_{\vec{k}}^{(1)}$, residing primarily on the down sublattice will gradually become excited. This results in a further preferential decrease of the down sublattice magnetization, and a falling behind of the up sublattice one. In fact, the initial decrease and the subsequent sign reversal of the effect of field on the up sublattice magnetization (Fig. 4) is a direct experimental confirmation of Bogolyubov coupling between the sublattices through zone-centered spin waves. It is also observed in Fig. 4 that the sign reversal is more pronounced the higher the field. This finds its origin in the fact that the splitting between the two magnon branches is larger when the magnetic field is increased.

The full curves in Fig. 4 represent the results of renormalized spin-wave theory, as in the case of the down sublattice magnetization without adjustment of the parameters, yielding an excellent fit to the data up to 20 K. At the lower fields ($\leq$ 10 kG) renormalization results in a minor improvement over the unrenormalized theory with the effective parameters (dashed lines in Fig. 4), in contrast to the higher fields where the breakdown of the unrenormalized theory occurs at 14 K in a field of 15 kG, and at 10 K in 20 kG. For comparison we also plotted the results of a calculation in the k^2 approximation and involving integration over k to infinity (dotted lines). Such a calculation appears to be grossly in error, and clearly indicates the necessity of exact integration over the complete Brillouin zone.

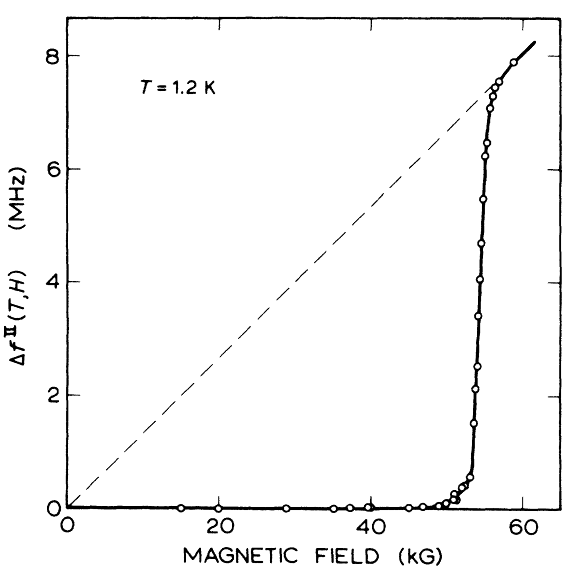

FIG. 5. Net magnetization at 1.2 K, as reflected in the NMR frequency of the in-layer $^{19}F^{II}$ nuclei corrected for the Zeeman shift $\Delta f^{II}(T,H)$ vs the magnetic field parallel to the c axis. The spin-flop transition is at 54.5 ± 0.5 kG.

C. Net magnetization

The NMR measurements at the $^{19}F^{II}$ nuclei, reflecting the net magnetization, differ in some important aspects from NMR at the $^{19}F^{I}$ sites. First, the magnetization-induced lineshifts of the $^{19}F^{II}$ nuclei are at least one order of magnitude smaller than the corresponding $^{19}F^{I}$ shifts. As a consequence, the $^{19}F^{II}$ resonance is much easier followed with temperature, and that without any loss in relative accuracy, since the experimental errors almost completely originate from the measurement of frequency rather than temperature. Secondly, the linewidth of the $^{19}F^{II}$ resonance near the transition is determined by fluctuations of the parallel susceptibility. Therefore, the linewidth increases only slightly at T_N,[13] and indeed the resonance can even be detected in going through the transition, in contrast to the $^{19}F^{I}$ resonance, whose linewidth goes with the staggered susceptibility and diverges near T_N. Similar conclusions may be drawn for the antiferromagnetic spin-flop transition (Fig. 5), but here it turns out to be

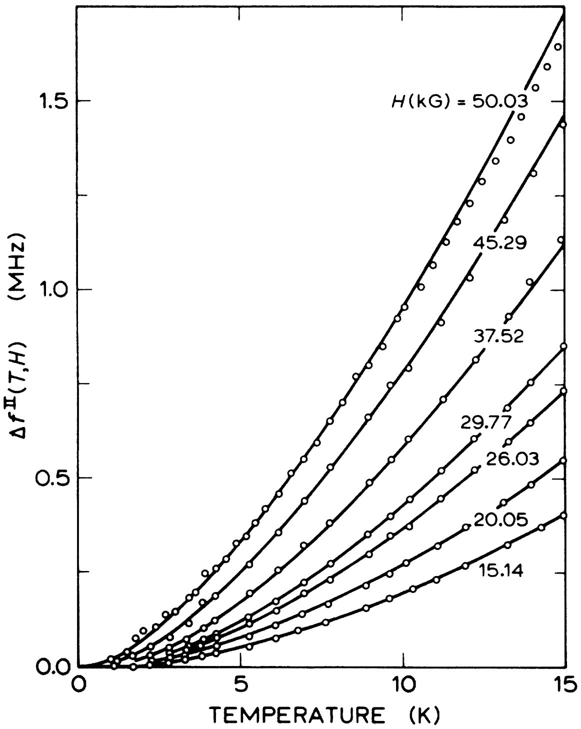

FIG. 6. Net magnetization, as reflected in the NMR frequency of the in-layer $^{19}F^{II}$ nuclei corrected for the Zeeman shift $\Delta f^{II}(T,H)$ vs temperature for various fields parallel to the c axis. Renormalized spin-wave theory (solid lines) has been adjusted to the data points below 30 kG and 15 K to determine the hyperfine coupling constant A_2.

important to properly align the tetragonal crystal axis along the external field. At 50 kG and 1.2 K we measured a linewidth of ~100 kHz for the $^{19}F^{II}$ resonance, as compared to 5 kHz at low fields. In addition, at 50 kG a zero-temperature lineshift of 110 kHz was observed, dropping steeply with decreasing field (Fig. 5), and apparently due to the vicinity of the spin-flop transition combined with a residual misalignment of the sample. Because such effects would scale with $\chi_\perp$, their minor contributions to the lineshift are expected to be nearly independent of temperature, and are subtracted from the data over the whole temperature regime. In an additional experiment with a larger misalignment we indeed found a larger zero-temperature lineshift, but the temperature dependence of the net magnetization, after subtraction of the above contribution, appeared to be the same.

The results of the $^{19}F^{II}$ resonance experiments are presented in Figs. 6 and 7, where a correction of ~4% due to demagnetizing fields is included. For the interpretation of the data the proportionality constant A_2+D_2 (see Sec. II) between the lineshift and the net spin momentum has to be known. Assuming spin-wave theory to be correct for low temperatures and fields, the low-magnetic-field data (≤ 30 kG) in the temperature range below 15 K (Fig. 6) have been fitted to renormalized spin-wave theory Eq. (18), with $J/k_B = -8.40$ K and $T_G(0) = 7.55$ K. We found $A_2+D_2 = -41.8 \pm 1.0$ MHz, which again includes the correction for the demagnetizing fields. With $D_2 = 9.4$ MHz (Sec. II), this yields for the transferred hyperfine constant $A_2 = -51 \pm 1$ MHz, which agrees with the NMR result in the paramagnetic regime $A_2 = -52 \pm 1$ MHz.[7]

With the value for A_2+D_2 obtained above, the spin-wave calculations, Eq. (18), have been extended to higher fields and temperatures (solid lines in Figs. 6 and 7), and compared with experiment. It is observed that for fields below 45 kG renormalized spin-wave theory agrees, within the experimental errors, with the data points up to

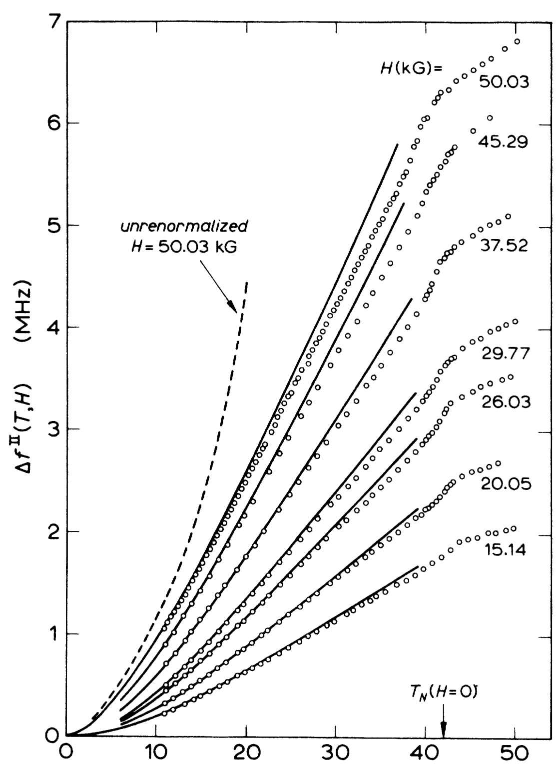

FIG. 7. Same as Fig. 6, but over a wider range of temperature. The part below 15 K is enlarged in Fig. 6. The solid lines are calculated from renormalized spin-wave theory, as described in text. The dramatic effect of renormalization is exemplified by the dashed curve representing unrenormalized theory at 50.03 kG with the effective parameters J_s and α_s. The change of T_N with field may be deduced from the variation of the inflection in the data near $T_N(H=0) = 42.1$ K.

18 K, but that even at the higher temperatures the maximum deviation between experiment and theory nowhere exceeds 3%. For the 45.29- and 50.03-kG series the point of breakdown between experiment and theory is reduced to 16 and 13 K, respectively. The results of unrenormalized theory with the effective parameters J_s and α_s are less impressive, with the temperature range of concurrence extending up to steadily decreasing temperatures when the field is increased. At 15 kG the range of agreement still extends up to 11 K, but decreases to only 4 K at 50 kG. The calculated unrenormalized result for 50.03 kG is shown as the dashed curve in Fig. 7, where it is noted that the dramatic improvement by renormalization mainly originates in the field-dependent term $p^{(1)} - p^{(2)}$ [Eq. (14)].

As discussed, at the highest fields, renormalized spin-wave theory starts to deviate from experiment at temperatures below 18 K, the point where the deviation starts at zero field. However, inspection of the calculations reveals that for *all* fields considered the breakdown occurs at a temperature where the thermal decrement of $\langle S_\uparrow^z \rangle$ is about 7% of the value at $T = 0$ K, as compared to 7% due to zero-point motion. As in zero field the conjecture is that at this point excitations set in that are not adequately treated by the usual expansion of the motion of spins in spin-wave theory. In this category fall critical fluctuations of the z component of the magnetization. While spin-wave theory accounts for the magnetization up to only ~45% of T_N, it appears that the phase boundary between the normal antiferromagnetic and the spin-flopped states can be approached very closely. Because of the considerable effect of the field-dependent renormalization, further agreement in the region near the spin-flop transition may perhaps be obtained by inclusion of $(1/2S)^2$ field-dependent renormalization in the magnon energies.

Finally, it is seen from Fig. 7 that the inflection point of the net magnetization versus temperature is moving towards lower temperatures upon increase of the field, from which the development of the antiferromagnetic-paramagnetic phase transition temperature may be deduced. At 30 kG the decrement of T_N is 1.1 ± 0.5 K, at 50 kG 3.5 ± 0.5 K.

V. CONCLUSIONS

We have investigated the sublattice and net magnetizations of the 2D antiferromagnet K_2MnF_4, with the following results. Spin-wave theory with the magnon energies renormalized with temperature and field throughout the entire Brillouin zone, as well as proper variation of the anisotropy with temperature, yields an excellent description for the temperature dependence of the sublattice magnetization below 18 K and up to 20 kG, the maximum field at which the resonance could be followed. With increasing field, renormalization, which in zero field yields a marginal improvement of 3 K over the unrenormalized theory, extends the regime of concurrence with spin-wave theory over increasingly larger temperature ranges, at 20 kG resulting in an extension from 10–18 K. This improvement over the unrenormalized calculation originates predominantly in the field-dependent renormalization, which is proportional to the difference between the occupations of the two magnon branches.

The net magnetization was followed up to fields of 50 kG, with the spin flop occurring at 54.5 kG at $T = 0$ K. The most remarkable and interesting point is that even at fields close to the spin flop the breakdown of renormalized theory does not occur much below the limit of 18 K. Another way of summarizing the limit of validity of renormalized spin-wave theory as a function of field and temperature is to say that the theory starts to deviate from experiment at a point in the (H, T) diagram where the *thermal* decrement of the sublattice magnetization is 7%, in addition to 7% due to zero-point motion. Apparently, the field-dependent part of the renormalization is quite well described by first-order Oguchi renormalized spin-wave theory, although a slight further improvement may possibly be obtained by incorporating $(1/2S)^2$ terms, whereas temperature-dependent renormalization does not adequately describe critical fluctuations associated with the transition to the paramagnetic state.

Another point of interest is that, starting from zero temperature, both the down and up sublattice magnetizations initially decrease more rapidly with temperature than in the zero-field case, in contrast to what one would expect from the molecular-field approach. The effect is more pronounced the higher the magnetic field, i.e., the larger the magnetic splitting between the magnon branches, and was discussed to be due to the preferential excitation of the long-wavelength magnons of the lower branch, which essentially reside on both sublattices. In other words, the effect provides direct experimental evidence of the Bogolyubov coupling of the sublattices.

Finally, experimental information was obtained on the hyperfine coupling of the in-layer $^{19}F^{II}$ nuclei, the field dependence of T_N, and the spin-flop field, whereby it was also demonstrated that NMR in the ordered state may be used advantageously to obtain these data.

ACKNOWLEDGMENT

The work is part of the research program of the Stichting voor Fundamenteel Onderzoek der Materie (FOM), and has been made possible by financial support from the Nederlandse Organisatie voor Zuiver Wetenschappelijk Onderzoek (ZWO).

---

[1]For a review, see L. J. de Jongh and A. R. Miedema, Adv. Phys. 23, 1 (1974).

[2]D. J. Breed, thesis (University of Amsterdam, 1969) (unpublished); Physica (Utr.) 37, 35 (1967).

[3]R. J. Birgeneau, H. J. Guggenheim, and G. Shirane, Phys. Rev. B 8, 304 (1973).

[4]H. W. de Wijn, L. R. Walker, and R. E. Walstedt, Phys. Rev. B 8, 285 (1973).

[5]R. E. Walstedt, H. W. de Wijn, and H. J. Guggenheim, Phys. Rev. Lett. 25, 1119 (1970).

[6]T. Oguchi, Phys. Rev. 117, 117 (1960).

[7]C. Bucci, G. Guidi, C. Vignali, V. Fano, and M. Giordano, Solid State Commun. 10, 1115 (1972).

[8]D. L. Decker and H. L. Laquer, Cryogenics 9, 481 (1969).

[9]H. W. de Wijn, L. R. Walker, S. Geschwind, and H. J. Guggenheim, Phys. Rev. B 8, 299 (1973).

[10]S. Foner, in *Magnetism*, edited by G. T. Rado and H. Suhl (Academic, New York, 1963), Vol. I, p. 383.

[11]T. Oguchi, Phys. Rev. 111, 1063 (1958).

[12]P. Pincus, Phys. Rev. 113, 769 (1959).

[13]C. Bucci and G. Guidi, Phys. Rev. B 9, 3053 (1974).